The Astrophysical Journal, 684:471–480, 2008 September 1

NEAR-INFRARED OBSERVATIONS OF THE TYPE Ib SUPERNOVA SN 2006jc: EVIDENCE OF INTERACTIONS WITH DUST

E. Di Carlo,[1] C. Corsi,[2] A. A. Arkharov,[3] F. Massi,[4] V. M. Larionov,[3,5]
N. V. Efimova,[3] M. Dolci,[1] N. Napoleone,[2] and A. Di Paola[2]
Received 2007 December 20; accepted 2008 May 9

ABSTRACT

In the framework of a program for the monitoring of supernovae in the near-infrared (NIR) carried out by the Teramo, Rome, and Pulkovo observatories with the AZT-24 telescope, we observed the supernova SN 2006jc in the *J*, *H*, and *K* photometric bands during a period of 7 months, starting ~36 days after its discovery. Our observations evidence a NIR rebrightening, peaking ~70 days after discovery, along with a reddening of $(H - K)$ and $(J - H)$ colors until 120 days after discovery. After that date, $(J - H)$ seems to evolve toward bluer colors. Our data, complemented with IR and optical observations found in the literature, show that the rebrightening is produced by hot, newly formed dust surrounding the supernova.

Subject headings: galaxies: individual (UGC 4904) — infrared: stars — supernovae: general — supernovae: individual (SN 2006jc)

1. INTRODUCTION

One of the main aims of the astronomical research on supernovae (SNe) has been the study of hydrogen-deficient objects, among them Type Ib SNe (helium-rich) and Type Ic SNe (helium-deficient; see Filippenko [1997] for a review of SN classification). These two subclasses of events are of great interest because, more than for all other types into which SNe have been classified, there are still many issues open about them, both in terms of observational properties and concerning their progenitors and the physics of the explosion. A number of different models have been proposed to account for the observed characteristics of SNe Ib/c. The most agreed-upon scenario is that of the core collapse (CC) of massive stars. It is now believed that their progenitors are Wolf-Rayet (WR) stars, i.e., highly evolved stars that have shed their H envelopes (or He envelopes, in the case of SN Ic progenitors) due to mass transfer in a binary system or by means of a stellar wind (for an updated review, see Crowther 2007). However, no observational evidence has been found to date allowing one to identify an explosion picture.

Since SNe are believed to be a major source of dust in galaxies (Todini & Ferrara 2001 and references therein), events showing signatures of interactions with circumstellar matter are of great interest to study how dust forms around these objects. In particular, near-infrared (NIR) observations until late epochs are instrumental in providing information on the ongoing processes. As an example, IR traces of dust condensation were found in the ejecta of SN 1987A starting ~500 days after the outburst (see, e.g., Bouchet & Danziger 1993). Unfortunately, good NIR light curves (LCs) spanning until late epochs are available only in a few cases. The observatories of Teramo (Italy), Rome (Italy), and Pulkovo (Russia) are involved in a program aimed at providing accurate LCs of SNe in the NIR (Di Carlo et al. 2002; Di Paola et al. 2002; Valentini et al. 2003) by using a dedicated 1 m class telescope equipped with a NIR camera. In the framework of this program, we present the results of our NIR follow-up of SN 2006jc, discovered on 2006 October 9.752 UT (Nakano et al. 2006) in the galaxy UGC 4904. The earliest photometric and spectroscopic observations (Crotts et al. 2006; Itagaki et al. 2006; Modjaz et al. 2006) identified the object as a peculiar Type Ib SN a few days past maximum light. The main feature of SN 2006jc in the NIR is a late rebrightening in the corresponding LCs, making SN 2006jc an intriguing event that gives us a huge opportunity for the study of dust formation around CC SNe and allows us to deepen our knowledge of how massive stars die.

Nakano et al. (2006) soon drew attention to an LBV-like luminous flare that had been detected in the same position as SN 2006jc 2 yr before. The spatial coincidence of the two events was carefully analyzed by Pastorello et al. (2007).

Both the character of the event and the preceding flare occurrence led many groups to carry out ground-based and satellite observations from many facilities and over a wide range of wavelengths, providing a wealth of data. Arkharov et al. (2006) were the first ones to note that the NIR brightness of the SN was undergoing a steady increase after the optical maximum, suggesting some kind of relation with dust. Immler et al. (2006) also suggested this, based on X-ray observations. It can be hypothesized that as a result of the LBV-like flare in 2004, a dense circumstellar medium originated, within which the SN exploded. However, LBV stars are supposed to be massive stars in a brief and unstable evolutionary phase from core H-burning to He-burning (WR stage). So, stellar evolution theories do not predict that a star in this phase can become a SN after only 2 yr or that a WR star would produce such a luminous eruption (Eldridge & Tout 2004; Heger et al. 2003). Pastorello et al. (2007) suggest as an alternative picture that the SN progenitor was part of a binary system and that the LBV-like eruption actually occurred in the companion star of the SN 2006jc progenitor. Nevertheless, the SN would have exploded in a dense circumstellar medium, as shown by the evidence of interactions with it. Tominaga et al. (2008) used the available observations from the X-ray to the optical, complemented by our NIR photometry, and modeled the event as the explosion of a WR star that was ~40 $M_\odot$ during its main-sequence phase. Dust carbonaceous grains would then have formed within the ejecta.

[1] Istituto Nazionale di Astrofisica — Osservatorio Astronomico Collurania-Teramo, Via Mentore Maggini, I-64100 Teramo, Italy; dicarlo@oa-teramo.inaf.it.
[2] Istituto Nazionale di Astrofisica — Osservatorio Astronomico di Roma, Via Frascati 33, I-00040 Monteporzio Catone (Roma), Italy.
[3] Central Astronomical Observatory at Pulkovo, Pulkovskoe Shosse 65, 196140 St. Petersburg, Russia.
[4] Istituto Nazionale di Astrofisica — Osservatorio Astrofisico di Arcetri, Largo Enrico Fermi 5, I-50125 Firenze, Italy.
[5] Astronomical Institute of St. Petersburg University, Petrodvorets, Russia.

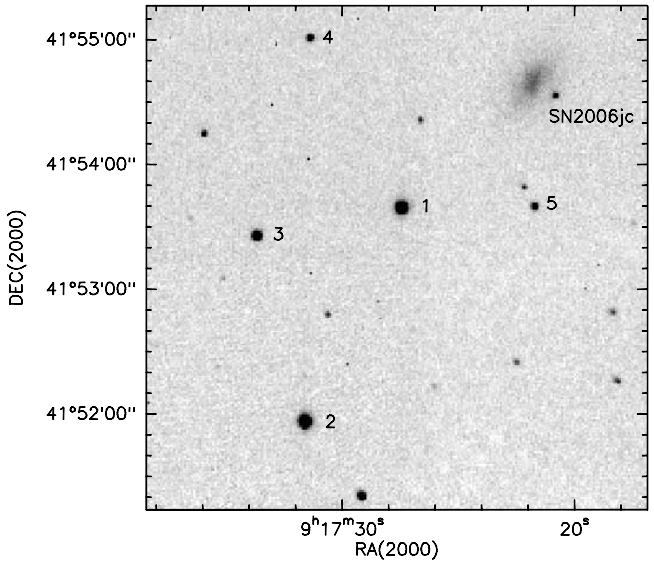

FIG. 1.—*J*-band image of SN 2006jc obtained at the AZT-24 telescope on JD 2,454,083. The stars of the local sequence are indicated by numbers.

This is one of the peculiarities of SN 2006jc, since a dust signature is hardly found in Type Ib/c SNe. One of the few instances of Ib SNe that dust may have been associated with is SN 1990I. However, in this case the presence of dust was only indirectly inferred from the optical data (missing NIR information) around day 250 (Elmhamdi et al. 2004). SN 2006jc is probably the very first instance of a Type Ib SN showing clear evidence of interaction with a dusty circumstellar environment, whether the dust is newly formed or preexisting.

The paper is organized as follows. We first describe the observations and data reduction (§ 2). Then we present the NIR LCs and color evolution of SN 2006jc and describe the construction of a bolometric (UVOIR) LC (§ 3). Finally, in § 4 we discuss the most likely origin of the NIR emission and its main constraints on the circumstellar medium.

2. OBSERVATIONS AND DATA REDUCTION

The observations of SN 2006jc were performed with the 1.1 m AZT-24 telescope at the Campo Imperatore Observatory (Italy), equipped with the NIR SWIRCAM camera (Brocato & Dolci 2003), which is based on a 256×256 HgCdTe NICMOS3 class array (PICNIC). The detector is sensitive to radiation in the spectral range from 0.9 to 2.5 μm and, at the focus of AZT-24, yields a scale of 1.04″ pixel^{-1}, resulting in a field of view of 4.4×4.4 arcmin^2.

A single set of observations in one of the *JHK* bands consists of three to five off-source images and five on-source images. During a night, for each band the number of sets acquired was selected based on the source brightness in that band. The on-source images in the same set were dithered with maximum shifts of 15″, and the individual integration times were 30 s. Off-source frames were offset by 20′ and were taken with the same observational procedure and exposure times as the on-source ones, but using a wider (30″) dithering. For each set, sky images were obtained as a median of the closest dithered off-source frames and subtracted from each on-source image in the same set.

A number of frames were acquired at twilight and used to obtain normalized flat-field images using the differential flat technique, as described in Di Carlo et al. (2002). Each sky-subtracted image was flat-field divided accordingly. To correct for residual low spatial frequency inhomogeneities in the system response over the frame, we used a set of observations of a standard star with many different pointings covering a grid of 7×7 regularly spaced positions on the detector area plus seven more positions at the center. For each of the 56 frames, a "sky" image was constructed by median filtering together the 12 frames closest to it in time. Each sky image was then removed from the corresponding frame, and the obtained images were corrected for flat-fielding. Aperture photometry of the standard star was carried out on each image, yielding a flux (in counts) as a function of the position on the grid. We fitted a second-degree polynomial to the grid and transformed it into a frame that, once normalized to the value at the centermost location, was used as a "superflat." Therefore, after flat-fielding, each frame was further divided by the superflat. The superflats evidenced large-scale smooth variations of at most $\sim$0.1 mag from the frame center to its edge. At last, the relevant scientific images were obtained by removing the bad pixels and finally registering and averaging together the dithered exposures using a 5 σ threshold.

Photometric observations in the *JHK* bands began on 2006 November 15, going on until 2007 June 6. The standard star AS 20 (Hunt et al. 1998) was observed to calibrate a sequence of secondary standards properly selected in the SN field among the ones with the highest signal-to-noise ratio (stars 1–5 in Fig. 1). We checked the calibrated magnitudes of the stars in the local sequence against the 2MASS catalog and found that they are in general within $\sim$0.02–0.04 mag of their 2MASS magnitudes. Only the two faintest ones exhibit larger differences in some of the band. Also, we found that the relative magnitudes of the local sequence remain constant within a few hundredths of a mag.

The magnitudes of SN 2006jc and the secondary standards in the field were obtained by point-spread function photometry using the ROMAFOT package (Buonanno et al. 1979). The procedure adopted to remove the contribution of the galaxy background

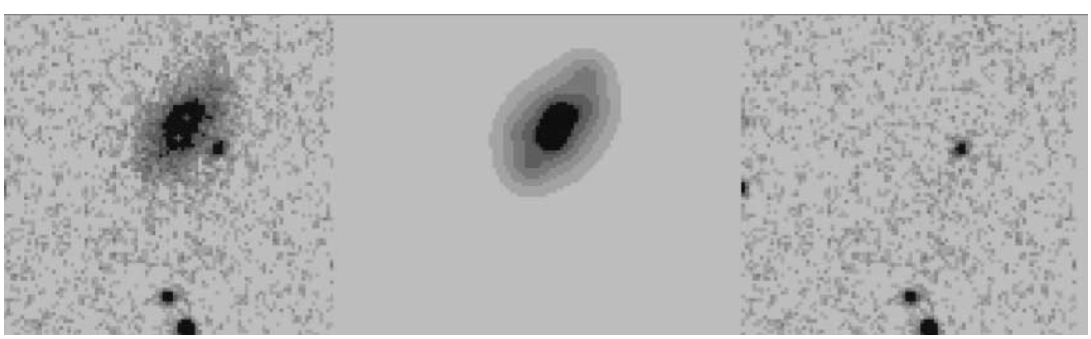

FIG. 2.—Sketch of the procedure used to remove the background contribution from the SN photometry. The region around the SN in the original image is shown in the left panel, and the same region after background subtraction is shown in the right panel. The subtracted contribution from the host galaxy has been modeled as a sum of six Gaussians (*middle panel*).

TABLE 1
NIR Photometry of SN 2006jc

Julian Date (2,454,000+)	J (mag)	ΔJ (mag)	H (mag)	ΔH (mag)	K (mag)	ΔK (mag)
54.6	16.16	0.04	15.68	0.04	15.12	0.03
55.6	...	...	15.64	0.04	...	...
62.6	...	...	...	...	14.74	0.04
63.6	16.03	0.05	15.54	0.03	...	...
72.6	16.12	0.05	15.24	0.02	14.45	0.04
75.6	16.05	0.04	15.07	0.02	14.27	0.02
76.6	16.09	0.05	...	...	...	...
77.6	...	...	15.00	0.02	14.17	0.02
82.7	15.95	0.06	14.78	0.02	13.96	0.02
83.7	15.96	0.04	14.75	0.02	14.03	0.02
132.3	17.67	0.17	15.99	0.03	14.78	0.02
137.3	17.64	0.15	16.23	0.03	14.94	0.03
159.4	18.18	0.31	...	...	15.22	0.04
162.4	...	...	16.75	0.05	15.46	0.10
164.4	18.77	0.38	16.83	0.03	15.32	0.05
165.5	18.74	0.33	...	...	15.35	0.05
168.4	...	...	...	...	15.42	0.06
172.4	18.90	0.40	16.80	0.02	15.48	0.05
173.4	...	...	16.87	0.02	15.43	0.06
174.4	...	...	16.89	0.02	15.30	0.07
175.4	18.84	0.48	17.0 8	0.04	15.62	0.12
176.4	...	...	16.96	0.03	15.54	0.11
177.4	...	...	17.04	0.02	15.61	0.09
181.3	...	...	...	...	15.58	0.11
197.4	18.86	0.50	17.45	0.17	15.91	0.09
202.3	18.98	0.51	17.78	0.28	16.13	0.11
207.3	19.06	0.72	...	...	16.25	0.13
219.3	...	...	...	...	16.51	0.11
226.3	...	...	...	...	16.53	0.11
235.2	...	...	...	...	16.68	0.11
258.3	...	...	...	...	17.58	0.21

Notes.—The isophotal wavelengths are $\lambda(J) = 1.250$ μm, $\lambda(H) = 1.644$ μm, and $\lambda(K) = 2.198$ μm; zero-magnitude fluxes are from Tokunaga & Vacca (2005).

diffuse emission is sketched in Figure 2 and consisted of modeling the galaxy by a set of several (five to eight) Gaussians with variable full width at half-maximum. The analytical reconstruction of the galaxy was subtracted from the original image, and the background residual around the SN was checked interactively. Finally, the SN photometry was carried out on the subtracted image showing the flattest background distribution. Table 1 lists the results of our photometry. The uncertainties due to photon statistics and fitting are also indicated.

3. RESULTS

3.1. *The NIR Light Curves*

The *JHK* LCs of SN 2006jc are shown in Figure 3. Unfortunately, no NIR data are available around the optical maximum, as the coverage started roughly 36 days after discovery. The NIR LCs span a period of about 7 months and exhibit a clear peak (the "rebrightening") around JD 2,454,083 or shortly after (i.e., 60–70 days after discovery) that is correlated with a slope decrease in the LCs at optical wavelengths (see Fig. 3). In ~30 days, H and K became brighter by at least 1 mag, whereas in J only a plateau was evident (or a small brightness increase, ~0.2 mag). Hence, the rebrightening mostly affected the NIR wavelengths, and its effects became smaller and smaller at shorter wavelengths. Then, while J and H faded by ~3 mag in 120 days, K dimmed by ~3.6 mag in 176 days. Note that the SN was brighter in K than it was in J and H, so it could be followed longer in this band. Two optical spectra taken around the rebrightening (Smith et al. 2008) exhibit a red continuum (along with a blue emission) that confirms excess emission in the NIR.

3.2. *NIR Color Evolution*

The evolution of the NIR colors ($J - H$ and $H - K$) is also shown in Figure 3. A reddening with time is evident, with ($H - K$) having steadily increased by ~1 mag in ~150 days, whereas ($J - H$) increased by ~1.6 mag in ~120 days and then decreased by ~1 mag, although with larger error bars, in the last ~30 days of the plotted color curve. The evolution of NIR colors can be better studied in a color-color diagram, where it can be compared with cooling and extinction of known stellar sources. In Figure 4, a NIR color-color plot is shown. The main sequence and its color evolution with increasing extinction are also drawn in the figure as key reference locations in the plot. If the NIR emission is mostly due to hot dust, the colors are expected to fall into a plot region below the reddening band of the main sequence, depending on dust temperature and extinction. In fact, the NIR colors of the SN mainly evolve below the main-sequence reddening band, along a track that is in practice parallel to the reddening vector. However, at the latest epochs plotted in the diagram, the blueing of ($J - H$) evidenced above causes the SN colors to move in a different direction, roughly perpendicular to an extinction vector. Although the errors in ($J - H$) become large at these late epochs, this change in color evolution might be real. Anyway, we are mainly concerned with the color evolution in the earlier phase shown in our diagram, i.e., during the rebrightening time, when the photometric errors are smaller.

This behavior in the NIR colors during the rebrightening is not only totally at odds with that of other nonstellar objects, like SNe Ia (e.g., Valentini et al. 2003), where dust is expected to play quite a marginal role in the light emission, but also different from, e.g., that of a "dusty" CC SN like the Type IIn SN 1999el (Di Carlo et al. 2002). In the latter case, dust is expected to be the main cause of the observed NIR excess, and, in fact, the NIR colors evolve below the reddening band of the stellar main sequence in an ($H - K$) versus ($J - H$) diagram. But the spread that it exhibits in the space of the colors is much less than in the case of SN 2006jc. Indeed, this evidence points to the fact that most of the NIR emission of SN 2006jc at the epochs considered in this work likely arises due to hot dust.

Two processes may then be envisaged to explain the reddening trend with time of the NIR colors: one where steady formation of dust in front of a NIR source causes a large increase with time of the extinction (referred to as the "pure extinction scenario" in the following), and the other where a hot (i.e., ~1000–2000 K) dust shell surrounding the SN, either newly formed or preexisting, cools (the "cooling dust scenario").

As for the first scenario, i.e., steady formation of dust in front of a NIR source, it leads to an extinction that is inconsistent with the optical and NIR LCs, and it can be discarded (see § 4). Nevertheless, it allows one to roughly derive an upper limit to the total mass of dust around the SN in the hypothesis of a spherically symmetric distribution of dust forming in the SN ejecta. From Figure 4, the track in the color-color diagram spans roughly $A_V = 15$ mag, and this can be assumed to be the maximum extinction that dust may cause. Assuming that the dust is homogeneously distributed in a spherical volume of radius R around the SN, its opacity τ_V, in the V band, is given by

$$\tau_V = \frac{3M_{\rm dust}}{4\pi R^2} k_V, \quad (1)$$

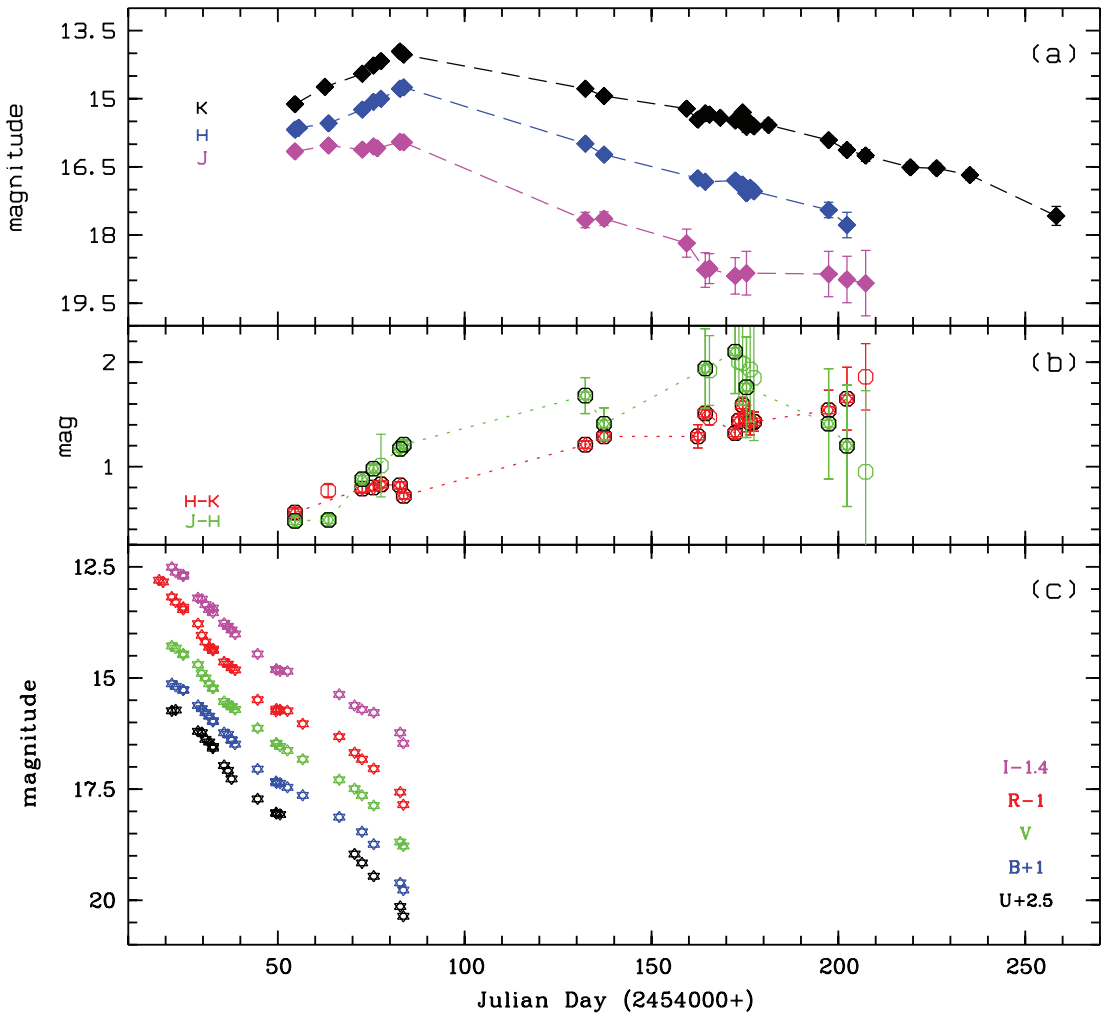

FIG. 3.—(*a*) NIR LCs and (*b*) the corresponding NIR colors [$(J - H)$ and $(H - K)$] of SN 2006jc. Partially filled hexagons correspond to epochs when photometry in all three bands is available, whereas open hexagons mark epochs when photometry in only two bands is available and has been complemented by interpolated values in the missing band. (*c*) To allow a more complete view of the NIR temporal evolution, the optical LCs (Pastorello et al. 2007) are also shown, shifted by the amount indicated in the lower right corner.

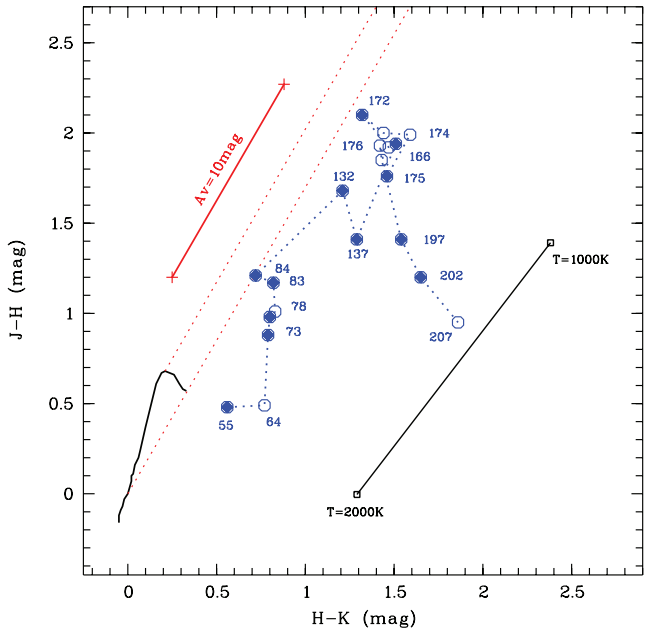

FIG. 4.—Color-color diagram [$(J-H)$ vs. $(H-K)$] showing the temporal evolution of SN 2006jc NIR colors. Each symbol is labeled with the corresponding epoch (JD 2,454,000+). Filled and open symbols are the same as in Fig. 3*b*. For the sake of clarity, error bars are omitted; however, they are plotted in Fig. 3. The stellar main sequence of O6–O8 to M8 stars (Koornneef 1983) is also drawn (*black line, lower left corner*), along with its reddening band (*red dashed lines*). The solid lines above and below the main-sequence reddening band mark, respectively, an extinction $A_V \sim 10$ mag and a blackbody cooling sequence from 2000 to 1000 K. Both of them are shifted by arbitrary intervals.

where k_V is the dust opacity per unit mass in the V band, $M_{\rm dust}$ is the total mass of dust, and $\tau_V = 1.086 A_V$. In the case of spherical dust grains, the opacity per unit mass is

$$k_V = \frac{3Q_V(a)}{4a\rho}, \qquad (2)$$

where a is the grain radius, Q_V is the grain absorption efficiency, and ρ is the mass density of a single grain. For small values of a (e.g., $a \lesssim 0.03$ μm for graphite grains), Q_V/a does not depend on a (Draine & Lee 1984). The absorption efficiency for small grains can be taken, e.g., from Draine (1985); in the case of $a = 0.01$ μm, Q_V is 7.57×10^{-2} for graphite and 5.69×10^{-3} for silicates. These values would be only a factor of 2 greater if $a = 0.1$ μm. We can also assume $\rho = 2.25$ g cm^{-3} for graphite and $\rho = 3.3$ g cm^{-3} for silicates (Draine 1985). Hence, k_V is strongly dependent on dust composition (2.3×10^4 cm^2 g^{-1} for graphite and 1.3×10^3 cm^2 g^{-1} for silicates). We can estimate $R = vt \sim 10^{16}$ cm, where v is the ejecta velocity and t is the time from the explosion (we adopted $v \sim 10{,}000$ km s^{-1} and $t \sim 200$ days). Using these values, from equation (1) we can derive upper limits for the total dust mass $M_{\rm dust}$ of 1.3×10^{-4} $M_\odot$ for graphite grains and 2.3×10^{-3} $M_\odot$ for silicate grains. If the dust were distributed within a shell at a distance R, $M_{\rm dust}$ would be a factor of 3 greater.

In the framework of the second scenario, the NIR emission would be due to cooling dust. We tested this scenario by deriving the NIR colors exhibited by hot dust distributed in a plane slab with constant density. In this case, it is easy to solve the transfer equation and obtain $I_\lambda(\lambda) = Q(\lambda) B_\lambda(T_d)(1 - e^{-\tau_\lambda})$, where $Q(\lambda)$ is the dust emission efficiency, $B_\lambda(T_d)$ is the brightness of a blackbody at the dust temperature T_d, and τ_λ is the dust optical depth at a wavelength λ. We can then use the Wien approximation and see that the NIR colors are given by

$$m_{\lambda_2} - m_{\lambda_1} = A(\lambda_1, \lambda_2, \tau_{\lambda_1}) + 1.086 \frac{hc}{kT_d}\left(\frac{1}{\lambda_2} - \frac{1}{\lambda_1}\right), \qquad (3)$$

where every dependence on dust properties and opacity now lies in the term A and, so, the dependence on T_d is explicit. Once "starting" colors are given (for any initial T_d, they are accounted for only in A), it is obvious that the cooling "sequence" causes a shift roughly in the same direction as the reddening vector. In particular, dust cooling from 2000 to 1000 K would cause $(H-K)$ to redden by 1.2 mag and $(J-H)$ by 1.5 mag, enough to account for the total change in NIR colors observed. This is also shown in Figure 4. The choice of the temperature interval is such as to roughly agree with the determinations of grain temperatures at different epochs discussed in the following. Furthermore, the upper limit is determined by the dust sublimation temperature, that is, $\sim$2000–3000 K (e.g., Draine & Hao 2002). To further check the cooling dust scenario, we fitted blackbody spectra to the *JHK* fluxes at different epochs. Since optically thin dust has emissivity $\sim\lambda^{-\beta}$, we also performed fits with modified blackbody (graybody) spectra, varying β in the range 1–2. The fits with pure blackbody curves are shown in Figure 5. Clearly, the temperature drops from $\sim$2900 K (JD 2,454,054.6) to $\sim$1200 K (JD 2,454,202.3). The modified blackbody fits give slightly worse results, although with temperature intervals from $\sim$2100–1700 to $\sim$1000 K. Since at early epochs a contribution from the much hotter SN photosphere is probably not negligible in the NIR fluxes, the obtained temperatures are in reasonable agreement with those inferred in the cooling dust scenario. The late color evolution, perpendicular to the reddening and the blackbody sequence, cannot be explained either by extinction or by dust cooling. The most likely cause is a major change in the geometry of the source, temperature gradients, and/or grain properties.

3.3. *Bolometric Light Curve*

We used our *JHK* photometry and the published *UBVRI* photometry, listed in Pastorello et al. (2007), to construct both a "UVOIR" (when the two data sets overlap) bolometric curve and a *UBVRI* (quasi-)bolometric LC. We assume a distance modulus of 25.8 ± 2.6 Mpc and a galactic extinction of $E(B-V) = 0.05$, as estimated by Pastorello et al. (2007). Measurements in all bands were first dereddened according to the extinction law from Cardelli et al. (1989), adopting $R_V = 3.1$ that gives $A_V = 0.155$ mag. The optical magnitudes were converted to fluxes according to Bessel (1979), while the NIR magnitudes were converted according to Tokunaga & Vacca (2005), following the standard of the UK Infrared Telescope (UKIRT). Note that ARNICA standards were defined using UKIRT standards (Hunt et al. 1998). We used spline fits to the LCs in order to have a homogeneous set of data at all wavelengths for each phase. The total flux at each epoch was computed by simply "connecting" the fluxes at the isophotal wavelengths and determining the total area. The results are listed in Table 2 and shown in Figure 6. The error on the derived bolometric luminosity is dominated by that on the distance and that due to the limited band used to calculate the total flux. As for the first, it is easy to see that it amounts to $\sim$20% of the bolometric luminosity. Being systematic, it causes a shift of the bolometric LC as a whole. The second contribution is more difficult to estimate, but it may be quite significant and may vary with time. However, it is likely to cause only small deformations

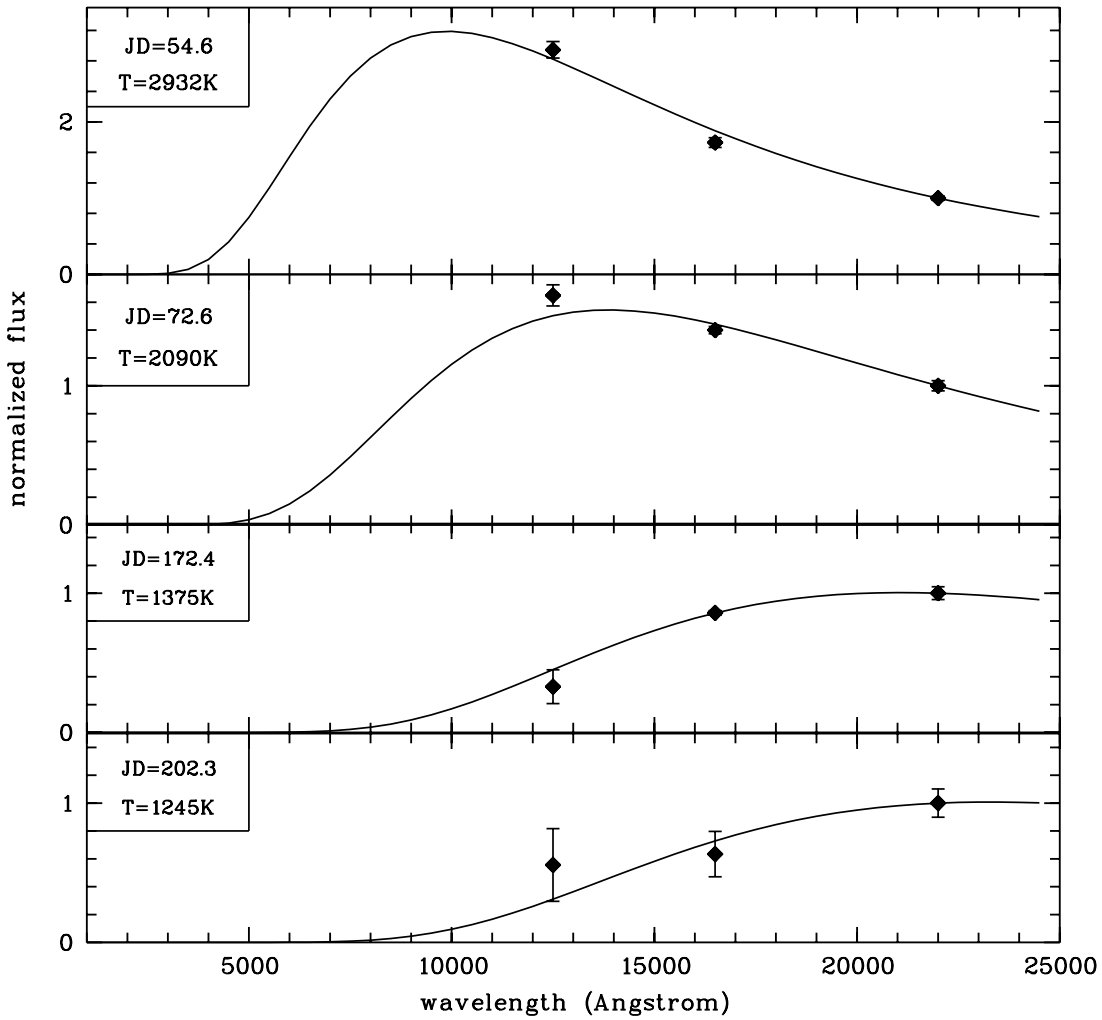

FIG. 5.—Blackbody spectra fitted to the *JHK* fluxes at four different epochs: the beginning of our NIR observations (JD 2,454,054.6), close to the NIR peak (JD 2,454,072.6), the end of the "cooling" sequence in the color-color diagram (JD 2,454,172.4), and one of the last observations (JD 2,454,202.3). The epoch and the best-fit temperature are indicated in the upper left corner of each panel. A drop in temperature from ~2900 to ~1200 K is evidenced.

TABLE 2
BOLOMETRIC LUMINOSITIES FOR SN 2006jc

Julian Date (2,454,000+)	$\log_{10}(L_{UBVRI})$ (erg s^{-1})	$\log_{10}(L_{\rm UVOIR})$ (erg s^{-1})
21.66.....	42.55	...
22.68.....	42.53	...
24.68.....	42.48	...
24.70.....	42.49	...
28.65.....	42.35	...
29.64.....	42.31	...
30.66.....	42.26	...
31.63.....	42.23	...
32.63.....	42.19	...
32.63.....	42.19	...
35.66.....	42.07	...
36.62.....	42.04	...
37.61.....	42.00	...
37.62.....	41.99	...
38.59.....	41.96	...
44.60.....	41.76	...
49.58.....	41.64	...
49.64.....	41.64	...
50.58.....	41.63	...
52.59.....	41.60	...
54.60.....	41.56	41.69
55.60.....	41.54	41.68
56.67.....	41.52	41.67
62.60.....	41.43	41.59
63.60.....	41.41	41.58
66.47.....	41.35	41.55
70.53.....	41.25	41.48
72.60.....	41.19	41.45
75.60.....	41.10	41.41
76.60.....	41.06	41.39
77.60.....	41.02	41.38
82.70.....	40.81	41.32
83.70.....	40.73	41.29

NOTES.—To derive L_{UBVRI}, fluxes have been integrated from 0.33 to 0.79 μm; to derive $L_{\rm UVOIR}$, fluxes have been integrated from 0.33 to 2.198 μm.

of the logarithmic bolometric LC, the major effect being a shift of the curve, as well. It is clear from the figure that the inclusion of the NIR fluxes changes the slope of the bolometric LC significantly, their contribution increasing with time from a factor of 1.35 to a factor of 3.6 of that from *UBVRI*.

Figure 6 also shows the bolometric luminosity obtained on JD 2,454,022.6 by adding the UV fluxes measured with *Swift* UVOT (Brown et al. 2006); the UV contribution amounts to ~80% of that from *UBVRI*. We roughly estimated the UV fluxes[6] on other dates from the figure shown in Holland et al. (2007). We found that the UV-to-optical *plus NIR* luminosity ratio appears to remain constant with time, although it is also roughly equal to the ratio of UV-to-optical luminosity as calculated at the discovery time, when NIR data are not available. Anyway, we decided not to scale the bolometric luminosity by including a constant contribution from UV emission, as we lacked a conclusive list of UV fluxes. The point marked in Figure 6 allows one to shift the bolometric LC as a whole if a constant fraction of UV contribution is assumed. The bolometric luminosities are derived by

[6] We used zero points, wavelengths, and count-to-flux ratios as given on the *Swift* Web site at http://heasarc.gsfc.nasa.gov/docs/heasarc/caldb/swift/docs/uvot/index.html. We also assumed $A_\lambda = A_U$ in all three UV bands to estimate the reddening correction for the UV flux.

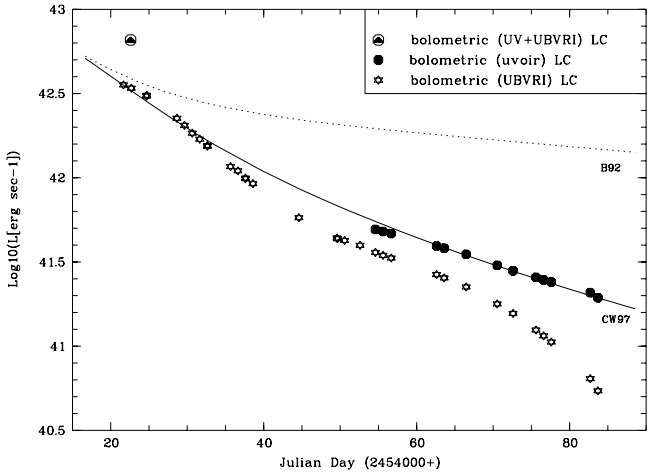

FIG. 6.—UVOIR bolometric LC and *UBVRI* (quasi-)bolometric LC, obtained by complementing the NIR data with optical photometry from Pastorello et al. (2007). The topmost point includes UV fluxes from Brown et al. (2006) to illustrate the UV contribution to the bolometric luminosity (see the text). Also plotted are the radioactive decay curve of ^{56}Ni and ^{56}Co (*dotted line*; Branch 1992) for an initial mass of 0.22 $M_\odot$ for ^{56}Ni (this is the expected LC if *all* the γ-rays are absorbed in the ejecta) and the same curve (*solid line*) for an initial mass of 0.22 $M_\odot$ for ^{56}Ni, but modified according to Clocchiatti & Wheeler (1997) to account for varying γ-ray trapping (by assuming a kinetic energy of 20×10^{51} erg s^{-1} and an ejecta mass of 4.6 $M_\odot$). In both cases, we adopt JD 2,454,005 as the explosion time.

assuming a constant reddening. In the next section we discuss the evidence for dust formation around the SN and increasing extinction. We show that L_{UBVRI} is actually affected by this increasing extinction. However, if all the UV-to-optical radiation absorbed by the dust is reemitted in the NIR, $L_{\rm UVOIR}$ will be unaffected by the increase in extinction. This point is also discussed in the following.

4. DISCUSSION AND CONCLUSIONS

Among the two proposed scenarios to explain the NIR color evolution, that of pure extinction can be easily ruled out. First, in the time interval when optical and NIR observations overlap, the extinction should have increased up to $A_V = 5$ mag. This can be easily estimated from Figure 4, exploiting the labeled dates. Since in this interval the increase in V is "only" ~2.5 mag, the background emitting region should have steadily increased its brightness to "compensate" for the remaining 2.5 mag of extinction. This can be obviously excluded. Second, even considering the much longer interval spanned by the NIR observations, the pure extinction scenario can be discarded on similar grounds. From Table 1 it can be seen that, e.g., K increased by ~2 mag from the epoch of the rebrightening peak to the latest dates plotted in the color-color diagram. Since on this timescale the extinction A_V should have increased by 15 mag, that translates into an increase of A_K by ~1.7 mag; then the growth of K would be fully explained by the extinction. Hence, the rebrightening would have again needed a source in the background of the newly formed dust whose NIR flux at first increased and then remained almost constant.

The simpler way to explain the NIR rebrightening is that the shock or the UV-optical radiation from the SN engulfed a distant dense shell of circumstellar matter from a past eruptive episode of the progenitor, either forming new hot dust in the dense post-shock gas or heating preexisting dust. Smith et al. (2008) show that if this eruptive episode is related to the 2004 flare event, then the shock would have reached the corresponding shell in ~100–200 days, comparable with the epoch of the rebrightening. Whereas

the bulk of the dust cooled behind, the shock or the UV-optical radiation would have yielded new layers of hot dust. We explored this possible mechanism by solving the transfer equation under the same assumptions as in § 3.2 but adding a plane-parallel outer layer of warmer dust around the emitting volume. If we adopt the reddening law by Rieke & Lebofsky (1985), then the *variation* of both *JHK* magnitudes and NIR colors depends only on the temperatures of the two regions and their opacities (in the *K* band). We checked that, by suddenly heating up the outer layer, a magnitude decrease of ∼1 mag (in the *JHK* bands) and a blueing in $(J - H)$, $(H - K)$ of only a few tenths of a magnitude can be yielded. This is just from using slightly different temperatures in the two regions (around 1500 K) and an optically thin outer envelope ($\tau_K \sim 0.1$). It is also noteworthy that an optically thin inner layer produces better results. This would agree with what was found by Foley et al. (2007), i.e., that there is little mass in the circumstellar medium, although there is evidence that it is quite dense. Our results are roughly consistent with both the *JHK* magnitude decrease and the $(H - K)$ behavior around the rebrightening epoch but fail to fit the apparent reddening of $(J - H)$ around the peak evident in Figure 4 [at $(H - K) \sim 0.8$, $(J - H) \sim 1.2$]. We also checked that two thicker layers ($\tau_K \sim 0.5$), the outer one being a little thicker and preexisting, would fit the data better, since now $(J - H)$ is reddened by a few tenths of a magnitude [along with $(H - K)$, which, however, is less reddened]. This may suggest that a shock proceeding in a moderately thick shell of circumstellar matter could fit the NIR data marginally better, although it does not agree with the estimated limit to the extinction. However, our two-layer model is too rough to help us decide which is the best selection of physical parameters. Accurate modeling, including dust properties (the adopted reddening law by Rieke & Lebofsky is not likely to fit newly formed grains) and the actual distribution of the circumstellar matter around the SN, is then needed to carefully investigate the proposed processes.

Sakon et al. (2007) observed SN 2006jc in the NIR and MIR with the Infrared Camera on board the *AKARI* satellite, 200 days after discovery. They showed that the 2–5 μm spectrum is well fitted by thermal emission from amorphous carbon grains at ∼800 K. Smith et al. (2008) also suggest that some observational evidence gathered roughly 79 days after discovery points to hot (∼1700 K) dust formation (carbonaceous grains) in a dense circumstellar shell engulfed by the shock. This confirms our scenario of dust cooling from ∼2000 to ∼1000 K. According to Sakon et al. (2007), their derived temperature 200 days after discovery is consistent with newly formed dust; the total mass in carbonaceous grains at that date has been estimated to be $\sim 7 \times 10^{-5}\ M_\odot$. This is of the same order of the upper limit as the dust mass we derive in § 3.2 and may suggest that dust is not distributed with spherical symmetry. However, by using the same grain properties as in Sakon et al. (2007), we obtain a slightly lower opacity (in the *K* band) than our estimated limit even in spherical symmetry.

Our NIR data alone do not allow us to discern between newly formed dust in dense postshock gas (or the ejecta) and heating of preexisting dust. But this issue can be addressed by comparing optical and NIR observations. In Figure 6 the curve of luminosity from the radioactive decay of ^{56}Ni and ^{56}Co has been drawn (Branch 1992) for an initial mass of $\sim 0.22\ M_\odot$ for ^{56}Ni. This process is believed to power the LC at late epochs. No wonder radioactive decay does not fit the slopes of the UVOIR and *UBVRI* (quasi-)bolometric curves, since an increasing escape probability of γ-rays with time is expected (Clocchiatti & Wheeler 1997). A simple model accounting for this effect in an expanding envelope has been developed by Clocchiatti & Wheeler (1997); it can be seen in Figure 6 that by modifying the radioactive decay curve by including the decrease of γ-ray trapping, we obtain a good fit to the UVOIR bolometric curve from JD 2,454,060 on. Here we have assumed an initial mass of $\sim 0.22\ M_\odot$ for ^{56}Ni, a kinetic energy of $\sim 20 \times 10^{51}$ erg s^{-1}, an ejecta mass of 4.6 $M_\odot$, and an explosion date of JD 2,454,005. These values are the same as the parameters derived by Tominaga et al. (2008) through one of their explosion models. However, note that our UVOIR curve does not include the UV contribution that appears to be a consistent fraction of the total radiated energy.

We draw attention to the clear steepening, or rather, the drop, of the *UBVRI* (quasi-)bolometric curve around JD 2,454,070 after it has been roughly parallel to the modeled bolometric curve for ∼20 days. This is obviously not matched by the UVOIR bolometric curve and reflects an analogous steepening of the *UBVRI* LCs around the same date (see Fig. 4). This has not been found in other Ib/c SNe, where the decline rate both of the *V*-band LC and the *UBVRI* (quasi-)bolometric curve, although larger than the slope of the radioactive decay curve, remains constant until a later epoch (Elmhamdi et al. 2004; Pastorello et al. 2007; Valenti et al. 2008); i.e., they are usually correlated to the radioactive decay curve (when γ-ray trapping is accounted for) until late epochs. The drop of the *UBVRI* curve is reminiscent of what was found for SN 1990I significantly later, around 250 days after maximum, and attributed to dust formation (Elmhamdi et al. 2004). Since in the case of SN 2006jc the *UBVRI* drop is well correlated with the rebrightening, in our view it also is the signature of incipient dust formation, occurring earlier than in the case of SN 1990I. The drop of the *UBVRI* (quasi-)bolometric curves is also evident in Figure 9 of Tominaga et al. (2008), where it clearly departs from their modeled bolometric curves from the same date on. Note that the analogous drop in the *I*-band LC is less than that in the *V*-band LC (see Fig. 4), as is expected from the extinction law. The amount of extinction at maximum *K* can be roughly derived by fitting a linear relation to the *UBVRI* (quasi-)bolometric curve in the period JD 2,454,050–2,454,070 and measuring the difference between the actual curve and this line. This implies $A_V \sim 0.5$ mag, or $\sim 4.5 \times 10^{-6}\ M_\odot$ of dust, assuming that small graphite grains are homogeneously distributed in a spherical volume of radius *R* (as defined in § 3.2). This value has to be increased by a factor of 3 if the dust is distributed in a thin shell around the SN. The derived masses are much lower than those involved in our pure extinction scenario, then consistent with its rejection. In Figure 7 we plot $(L_{\rm UVOIR} - L_{UBVRI})$, i.e., the NIR luminosity. This is compared with the difference between the total luminosity from the radioactive decay (Branch 1992; assuming an initial mass of 0.22 $M_\odot$ for ^{56}Ni) and L_{UBVRI}. If the NIR luminosity is totally contributed by hot dust, the latter represents the total luminosity of γ-rays escaping from the ejecta. It is noteworthy that $L_{\rm UVOIR} - L_{UBVRI}$ declines until JD 2,454,070 and then increases. The decline is probably dominated by the natural decline of the SN LC, whereas the increasing part marks a growing contribution from hot dust. If this is the case, then we can use equation (3) of Smith & Gehrz (2005) to derive the total mass of small carbon grains, assuming a temperature of 1600 K. The obtained values are listed in Table 3. Note that these values have to be increased to account for the IR emission at $\lambda > 2.2$ μm; e.g., by integrating blackbody emission at 1600 K, we can estimate this correction to be roughly a factor of 3. Clearly, at JD 2,454,070 the dust mass is $\sim 4.9 \times 10^{-6}\ M_\odot$, which, once corrected by a factor of 3, is consistent with the value derived above from the drop of L_{UBVRI} if the dust is distributed in a shell.

Figure 7 also shows the fraction of escaping γ-rays as derived from the difference between the luminosity from the radioactive decay and L_{UBVRI} compared with that predicted by the simple

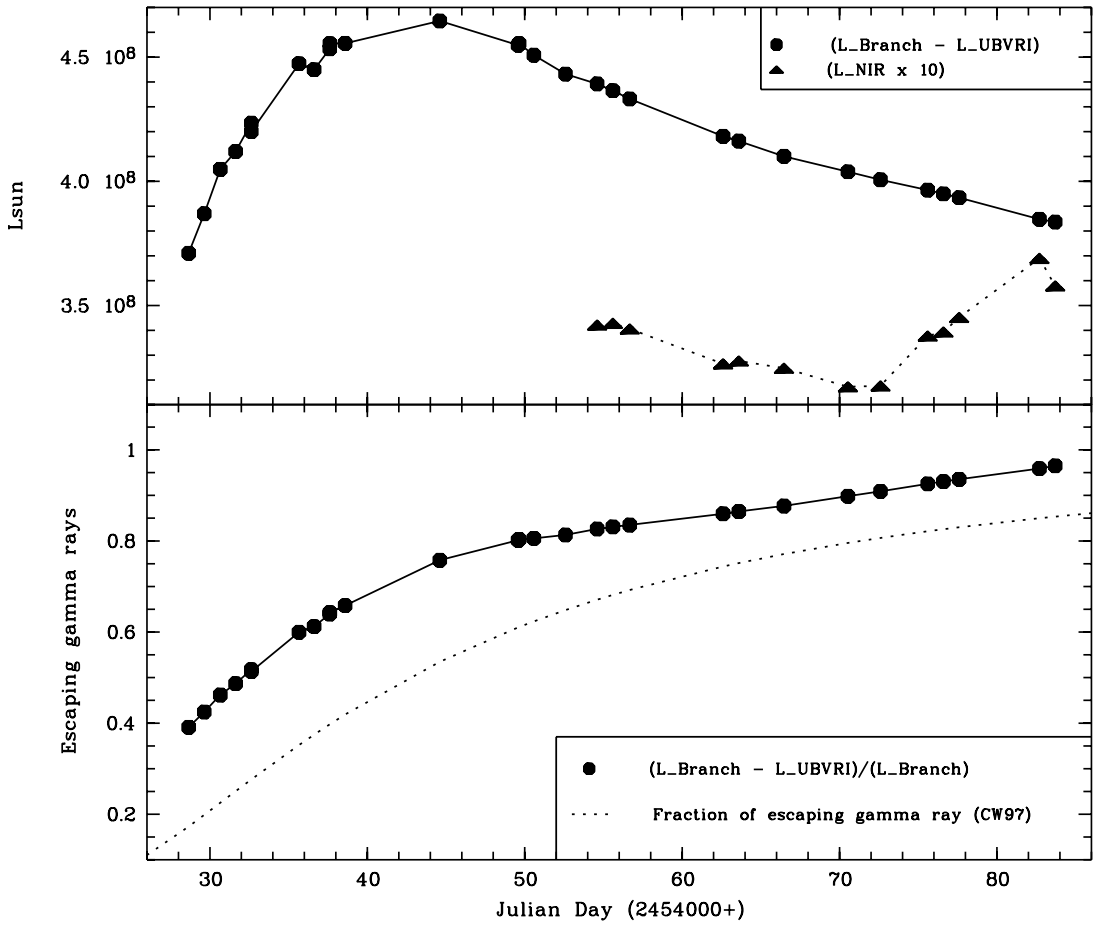

FIG. 7.—*Top*: Difference between the luminosity from the radioactive decay (Branch 1992; for an initial mass of 0.22 $M_{\odot}$ for ^{56}Ni) and L_{UBVRI} (*solid line*), i.e., the escaping γ-ray luminosity. The dotted line indicates $[(L_{\rm UVOIR} - L_{UBVRI}) \times 10]$, i.e., the NIR luminosity. *Bottom*: Escaping γ-ray luminosity (*solid line*) shown in the top panel divided by the luminosity from the radioactive decay. The dotted line shows the fraction of escaping γ-rays ($e^{-\tau_\gamma}$) according to Clocchiatti & Wheeler (1997).

model by Clocchiatti & Wheeler (1997). As expected, the former overestimates the fraction of escaping γ-rays, since we do not include in L_{UBVRI} the contribution from the UV emission. A change of slope is evident around JD 2,454,050 that is not matched by the theoretical curve. This roughly marks the onset of the NIR rebrightening and might just suggest that some of the assumptions made by Clocchiatti & Wheeler (1997), e.g., regarding the geometry of the envelope expansion, are no longer valid from this epoch on.

If the dust absorbs part of the UV-optical radiation from the ejecta and reemits it in the NIR, and if this is the only source of energy for the NIR emission, then it is easy to see that $\langle\tau\rangle = \ln(L_{\rm UVOIR}/L_{UBVRI})$. We checked that for optical thin dust and a flat UV-optical spectrum, $\langle\tau\rangle$ only slightly underestimates τ_V; then we can assume $A_V = 1.086 \ln(L_{\rm UVOIR}/L_{UBVRI})$. We have listed the values obtained in this way in Table 3. On JD 2,454,070, A_V is consistent with that obtained from the drop of L_{UBVRI}. Actually, $L_{\rm UVOIR}$ should be increased to account for the flux at $\lambda > 2.2$ μm and, along with L_{UBVRI}, also increased to account for the UV flux. We already estimate these correcting factors to be $\sim$3 for $L_{\rm UVOIR} - L_{UBVRI}$ (dust at 1600 K) and 1.8 for $L_{\rm UVOIR}$ (UV missing flux). Since $L_{\rm UVOIR}$ is dominated by the NIR emission, L_{UBVRI} should actually be increased by more than a factor of 1.8 to account for the UV flux. However, if the dust is distributed in a thin shell, we should also "shift" L_{UBVRI} in the above formula to account for the time needed for the light to reach the shell ($\sim$4 days for a radius $R \sim 10^{16}$ cm). Table 3 also lists the values obtained by shifting L_{UBVRI} 5 days forward on the time axis. Obviously, A_V is now smaller, and this partially compensates for the increase due to the luminosity corrections.

TABLE 3

TOTAL MASS OF DUST AND EXTINCTION AS DERIVED FROM THE SN LUMINOSITIES IN DIFFERENT WAVELENGTH INTERVALS

Julian Date (2,454,000+)	$M_{\rm dust}$ (10^{-6} $M_{\odot}$)	A_V[a] (mag)	A_V[b] (mag)
70.53.....	4.9	0.6	...
72.60.....	4.9	0.6	...
75.60.....	5.2	0.8	0.4
76.60.....	5.2	0.8	...
77.60.....	5.3	0.9	0.5
82.70.....	5.7	1.3	0.7
83.70.....	5.5	1.4	...

NOTE.—Also see the text.
[a] Uncorrected for light travel time.
[b] Corrected for a light travel time of 5 days.

The discussion above gives important clues about the energy source fueling the rebrightening. As shown, the UVOIR bolometric curve appears to be consistent with the curve of radioactive decay, once modified by including the simple γ-ray trapping model developed by Clocchiatti & Wheeler (1997). This would be in accord with Tominaga et al. (2008), who propose the radioactive decay as the major energy input powering the LCs. But it also naturally agrees with the picture in which the dust just

reemits the absorbed fraction of UV-optical radiation from the ejecta in the NIR.

In summary, we have presented the results of our NIR follow-up of SN 2006jc. This has evidenced a rebrightening of the *JHK* LCs that is coincident with a drop in the *UBVRI* LCs taken from the literature. We have shown that the data are consistent with hot, newly formed dust whose mass increases with time. The high dust temperature, close to the sublimation limit, may be better understood in a scenario of dust formation rather than shock heating of preexisting dust. In the first case, dust would just start to form when grains attain a low enough temperature, explaining why it is close to its allowed maximum already at the beginning of the NIR rebrightening. In the second case, the properties of the shock and gas and the distance of the shocked shell should be such as to coincidentally yield dust heating just below the sublimation limit. Along with the progressive fading of the redshifted side of intermediate-width He I emission lines found by Smith et al. (2008), the UV-to-NIR data make the case for early dust formation around SN 2006jc compelling. We have also shown that the NIR emission is naturally explained as arising due to dust heated by the UV-optical radiation from the ejecta. Whether the dust formed in the postshock gas, as convincingly proposed by Smith et al. (2008), or in the ejecta can be assessed only through detailed modeling of all the spectral and photometric data available. A brightening of X-ray emission from $\sim$20 to $\sim$100 days after discovery has been interpreted by Immler et al. (2008) as the result of the SN shock with a dense shell of material, consistent with that believed to be released by an outburst of the progenitor. The X-ray brightening occurred during the NIR rebrightening; hence, the interaction between ejecta and outer shell arose at the same epoch as dust formation. If not merely coincidental, this timing suggests some relation between dust formation and the shock passing the dense shell. A scenario where dust forms in the postshock gas would allow continuous formation of layers of hot dust, whereas the bulk of the dust behind, heated by the UV-optical radiation from the ejecta, slowly cools. We showed that a two-layer model would be consistent with both the NIR rebrightening and the evolution of the NIR colors.

We wish to thank Amedeo Tornambé for discussions, suggestions, and encouragement at all stages of this work. We thank M. Limongi and N. Tominaga for their kindly collaboration. We also thank an anonymous referee, whose comments improved the quality of this paper. This work is supported by governmental grant PRIN-MIUR 2006 under the scientific project "Fasi finali dell'evoluzione stellare—Nucleosintesi in Supernovae." This publication makes use of data products from the Two Micron All Sky Survey, which is a joint project of the University of Massachusetts and the Infrared Processing and Analysis Center, California Institute of Technology, funded by the National Aeronautics and Space Administration and the National Science Foundation.

REFERENCES

Arkharov, A., Efimova, N., Leoni, R., Di Paola, A., Di Carlo, E., & Dolci, M. 2006, Astron. Tel., 961, 1
Bessel, M. S. 1979, PASP, 91, 589
Bouchet, P., & Danziger, I. J. 1993, A&A, 273, 451
Branch, D. 1992, ApJ, 392, 35
Brocato, E., & Dolci, M. 2003, Mem. Soc. Astron. Italiana Suppl., 74, 110
Brown, P. J., Immler, S., & Modjaz, M. 2006, Astron. Tel., 916, 1
Buonanno, R., Corsi, C. E., De Biase, G. A., & Ferraro, I. 1979, in Proc. International Workshop on Image Processing in Astronomy, ed. G. Sedmak, M. Capaccioli, & R. J. Allen (Trieste: Osserv. Astron. Trieste), 354
Cardelli, J. A., Clayton, G. C., & Mathis, J. S. 1989, ApJ, 345, 245
Clocchiatti, A., & Wheeler, J. C. 1997, ApJ, 491, 375
Crotts, A., Eastman, J., Depoy, D., Prieto, J. L., & Garnavich, P. 2006, Cent. Bur. Electron. Tel., 672
Crowther, P. A. 2007, ARA&A, 45, 177
Di Carlo, E., et al. 2002, ApJ, 573, 144
Di Paola, A., et al. 2002, A&A, 393, L21
Draine, B. T. 1985, ApJS, 57, 587
Draine, B. T., & Hao, L. 2002, ApJ, 569, 780
Draine, B. T., & Lee, H. 1984, ApJ, 285, 89
Eldridge, J. J., & Tout, C. A. 2004, MNRAS, 353, 87
Elmhamdi, A., Danziger, I. J., Cappellaro, E., Della Valle, M., Gouiffes, C., Phillips, M. M., & Turatto, M. 2004, A&A, 426, 963
Filippenko, A. V. 1997, ARA&A, 35, 309
Foley, R. J., Smith, N., Ganeshalingam, M., Li, W., Chornock, R., & Filippenko, A. V. 2007, ApJ, 657, L105
Heger, A., Fryer, C. L., Woosley, S. E., Langer, N., & Hartmann, D. H. 2003, ApJ, 591, 288
Holland, S., Immler, S., Brown, P. J., Roming, P. W. A., vanden Berk, D., & Milne, P. A. 2007, in AIP Conf. Proc. 937, Supernova 1987A: 20 Years After: Supernovae and Gamma-Ray Bursters, ed. S. Immler, K. W. Weiler, & R. McCray (New York: AIP), 391
Hunt, L. K., Mannucci, F., Testi, L., Migliorini, S., Stanga, R. M., Baffa, C., Lisi, F., & Vanzi, L. 1998, AJ, 115, 2594
Immler, S., Modjaz, M., & Brown, P. J. 2006, Astron. Tel., 934, 1
Immler, S., et al. 2008, ApJ, 674, L85
Itagaki, K., et al. 2006, IAU Circ. 8762
Koornneef, J. 1983, A&A, 128, 84
Modjaz, M., Blondin, S., Kirshner, R., Challis, P., Matheson, T. & Mamajek, E. 2006, Cent. Bur. Electron. Tel., 676
Nakano, S., Itagaki, K., Puckett, T., & Gorelli, R. 2006, Cent. Bur. Electron. Tel., 666
Pastorello, A., et al. 2007, Nature, 447, 829
Rieke, G. H., & Lebofsky, M. J. 1985, ApJ, 288, 618
Sakon, I., et al. 2007, ApJ, submitted (arXiv: 0711.4801)
Smith, N., Foley, R. J., & Filippenko, A. V. 2008, ApJ, 680, 568
Smith, N., & Gehrz, R. D. 2005, AJ, 129, 969
Todini, P., & Ferrara, A. 2001, MNRAS, 325, 726
Tokunaga, A. T., & Vacca, W. D. 2005, PASP, 117, 421
Tominaga, N., et al. 2008, ApJ, in press (arXiv: 0711.4782)
Valenti, S., et al. 2008, MNRAS, 383, 1485
Valentini, G., et al. 2003, ApJ, 595, 779